

HIGH AVERAGE BRILLIANCE COMPACT INVERSE COMPTON LIGHT SOURCE*

K. Deitrick[†], J.R. Delayen¹, G.A. Krafft¹,

Center for Accelerator Science, Old Dominion University, Norfolk VA, 23529, USA

¹ also at Thomas Jefferson National Accelerator Facility, Newport News VA, 23606, USA

Abstract

There exists an increasing demand for compact Inverse Compton Light Sources (ICLS) capable of producing substantial fluxes of narrow-band X-rays. While multiple design proposals have been made, compared to typical bremsstrahlung sources, most of these have comparable fluxes and improve on the brilliance within a 0.1% bandwidth by only a few orders of magnitude. By applying cw superconducting rf beam acceleration and rf focusing to produce a beam of small emittance and magnetic focusing to produce a small spot size on the order of a few microns at collision, the source presented here provides a 12 keV X-ray beam which outperforms other compact designs and bremsstrahlung sources. Compared to a bremsstrahlung source, the flux is improved by at least an order of magnitude and the average brilliance by six orders of magnitude. Surpassing other compact ICLS designs, the source presented here is attractive to a wide variety of potential users.

INTRODUCTION

Inverse Compton Light Source

An Inverse Compton Light Source uses inverse Compton scattering to produce X-rays (or γ -rays, at higher energies), by colliding a relativistic electron beam and an incident laser. For a head-on collision between the two beams in the Thomson regime, the X-rays scattered in the forward direction (in the same direction as the electron beam) have the highest energy. The energy of these X-rays is given by

$$E_{X\text{-ray}} = 4\gamma^2 E_{\text{laser}} \quad (1)$$

where γ is the relativistic Lorentz factor of the electron beam and E_{laser} is the energy of the incident laser. The total number of the scattered photons is given by

$$N_\gamma = \sigma_T \frac{N_e N_{\text{laser}}}{2\pi(\sigma_e^2 + \sigma_{\text{laser}}^2)} \quad (2)$$

where σ_T is the Thomson cross section $8\pi r_e^2/3$, r_e is the classical electron radius, N_e is the number of electrons in the bunch, N_{laser} is the number of photons in the laser, σ_e is the spot size of the electron beam, and σ_{laser} is the number of photons in the laser pulse. For a high repetition rate source, the full flux of the X-ray beam is given by $\mathcal{F} =$

fN_γ , with f being the repetition rate. The flux into a 0.1% bandwidth is given by

$$\mathcal{F}_{0.1\%} = 1.5 \times 10^{-3} f N_\gamma. \quad (3)$$

For the source presented, and others also in the non-diffraction limited mode of operation, the average brilliance of the X-ray beam is given by

$$\mathcal{B} = \frac{\gamma^2 \mathcal{F}_{0.1\%}}{4\pi^2 \epsilon_{x,rms}^N \epsilon_{y,rms}^N} \quad (4)$$

where γ is the relativistic factor of the electron beam and $\epsilon_{x,rms}^N$ and $\epsilon_{y,rms}^N$ are the appropriate transverse normalized rms emittances of the electron beam [1].

Design Considerations

When designing a compact ICLS, three factors are critical. The machine should be small - one suggested limit was occupying a footprint of less than 100 m^2 [2]. The cost to purchase and operate the light source should be reasonable for smaller facilities. Finally, the parameters of the X-ray beam should demonstrate a significant improvement over traditional bremsstrahlung sources [3]. The parameters for this design were inspired by [4].

Accordingly, the frequency of the superconducting rf (srf) components which comprise the accelerator have been chosen to have a frequency of 500 MHz. This frequency allows for the machine to operate at 4 K, significantly reducing the cryogenic costs associated with operating the light source. In order to limit the size of the machine, every effort was made to develop a compact design without sacrificing the quality of the X-ray beam. Finally, the anticipated X-ray beam of this design far exceeds typical bremsstrahlung sources and shows improvement over other compact ICLS designs. The design presented here consists of an srf reentrant gun, four srf double-spoke cavities which make up the linac, and three quadrupoles to make up the focusing section [3].

Simulation Tools

This light source design was developed through extensive start-to-end simulation work. The electromagnetic (EM) fields of the srf reentrant gun were calculated using Superfish [5], while the EM fields of the srf double-spoke cavities in the linac were calculated using CST Microwave Studio [6]. Using IMPACT-T [7], 100,000 macroparticles were tracked through the accelerator, before being tracked through the focusing section by elegant [8].

* Partially authored by Jefferson Science Associates, LLC under U.S. DOE contract NO. DE-AC05-60R23177.

[†] kdeit001@odu.edu

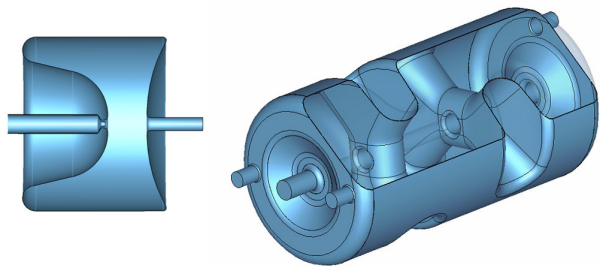


Figure 1: A cross section of the srf gun (left) and the srf double-spoke accelerating cavity (right).

ICLS DESIGN

Srf Reentrant Gun

The concept for a reentrant srf gun was introduced over 20 years ago [9]. In the last decade, the Naval Postgraduate School, Brookhaven National Lab, and the University of Wisconsin have commissioned reentrant srf guns [10]. For the design presented here, the gun needed to produce an electron bunch with extremely small transverse normalized *rms* emittances. This goal was achieved by altering the geometry of the gun, shown at the left in Fig.1, specifically around the nose-cone containing the cathode assembly. The geometry alteration resulted in radial electric fields within the gun, which provided focusing to the bunch in order to provide emittance compensation for the space charge effects [11]. Other srf reentrant gun designs use a solenoid for emittance compensation, instead of the rf focusing used here [10].

Srf Linac

Until recently, accelerating electrons near the speed of light has not been attempted with multispoke cavities, largely due to the well-established and successful performance of TM-type cavities. However, they are familiar options for accelerating ions and provide the capability to operate at 4 K through a low-frequency accelerator. The double-spoke cavity which makes up the linac, seen at the right in Fig.1, was designed by Christopher Hopper during his PhD research at Old Dominion University [12, 13].

The linac contains four of these double-spoke cavities. Due to the multipole effects of these cavities, some consideration was necessary to produce a nearly round electron beam at the linac exit. The multipole effects of the cavities can be approximated as “quadrupole-like”, focusing in one transverse direction while defocusing in the other. In order to produce a nearly round beam, the center two cavities within the linac were rotated 180° around the *y*-axis. While the produced beam is not perfectly round, it is close enough to make focusing the beam easier [11].

02 Photon Sources and Electron Accelerators

A23 Other Linac-based Photon Sources

Table 1: Properties of Electron Bunch at the Collision Point

Parameter	Quantity	Units
kinetic energy	25	MeV
bunch charge	10	pC
<i>rms</i> energy spread	3.44	keV
$\epsilon_{x,rms}^N$	0.10	mm-mrad
$\epsilon_{y,rms}^N$	0.13	mm-mrad
σ_x	3.4	μm
σ_y	3.8	μm
FWHM bunch length	3	psec
σ_z	0.58	mm

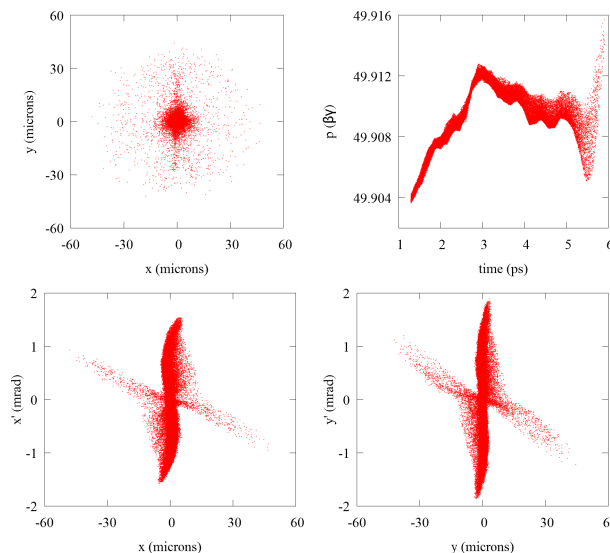


Figure 2: The beam spot (upper left), longitudinal phase space (upper right), horizontal phase space (lower left), and vertical phase space (lower right) of the electron bunch at the collision point.

Focusing

After the bunch exits the linac, it passes through three quadrupoles. The collision between the electron beam and the laser, known as the interaction point, occurs 29 cm past the exit of the last quadrupole. Due to an appropriate choice in bunch length off the cathode, no bunch compression is necessary, which significantly simplifies the design. The properties of the electron bunch at the interaction point are given in Table 1. The entire length from the surface of the cathode to the interaction point is less 6 m. The electron bunch distribution, which has been tracked from the cathode surface to the collision point, is shown in Fig. 2 [11].

X-RAY YIELD

The intended incident laser for this project is one with 1 MW of circulating power, a spot size of 3.2 μm , and a wavelength of 1 μm . Using the formulae presented at the

ISBN 978-3-95450-182-3

Table 2: X-ray Source Properties, Using Formulae

Parameter	Quantity	Units
E_x	12	keV
\mathcal{F}	1.4×10^{14}	ph/sec
$\mathcal{F}_{0.1\%}$	2.1×10^{11}	ph/(s-0.1%BW)
\mathcal{B}	1.0×10^{15}	ph/(s-mm ² -mrad ² -0.1%BW)

beginning of this paper, the anticipated X-ray properties can be calculated; these results are given in Table 2 [11]. However, these formulae were developed under the assumption that the electron beam distribution is Gaussian, which is not the case here [1, 11]. A recent work ([3]) provides the means to calculate the scattered photon spectrum for specific electron distributions, such as those provided by a start-to-end simulation. Using this method, the anticipated brilliance for this design is $\sim 9.4 \times 10^{14}$ ph/(s-mm²-mrad²-0.1%BW), which is close to the brilliance given by the formulae [3, 11].

It is important to give some perspective to these numbers. The best rotating anodes currently in use have a flux of $\sim 10^9$ ph/s and a brilliance on the order of 10^9 ph/(s-mm²-mrad²-0.1%BW) [22]. On the other hand, an X-ray beam that might typically be found at a large synchrotron or free-electron laser (FEL) facility may have a flux of $\sim 10^{11} - 10^{13}$ ph/s [23] with a brilliance of $\sim 10^{19}$ ph/(s-mm²-mrad²-0.1%BW) [24]. Table 3 contains anticipated X-ray properties of various compact ICLS projects.

Table 3: Comparison of X-ray Beam Parameters for Different ICLS Compact Designs

Project	E_x (keV)	Ph/s	Ph/(s-mrad ² -mm ² -0.1%BW)
Lyncean [1, 14, 15]	10-20	10^{11}	10^{11}
TTX [16]	20-80	10^{12}	10^{10}
LEXG [17]	33	10^{13}	10^{11}
ThomX [18]	20-90	10^{13}	10^{11}
KEK QB [19]	35	10^{13}	10^{11}
KEK ERL [20]	67	10^{13}	10^{11}
NESTOR [21]	30-500	10^{13}	10^{12}
MIT [22]	12	10^{13}	10^{12}
ODU	12	10^{14}	10^{15}

While all the projects listed in Table 3 produce X-rays beams with a flux comparable to what may be found at large facilities, the anticipated brilliance falls significantly short. The reason that the large facilities have such a high brilliance is because the electrons are high energy. Other compact projects do improve on brilliance when compared to a traditional X-ray source; the design presented here has

a greater brilliance by orders of magnitude than the next most brilliant proposal. Furthermore, there is nothing to stop this design from being further optimized to produce an even more impressive X-ray beam.

CONCLUSION

The compact Inverse Compton Light Source presented here is a world-class X-ray source, anticipating a brilliance unmatched by traditional sources or other compact ICLS designs. This brilliance is achieved by an extremely small transverse normalized *rms* emittance, which has been achieved by a srf reentrant gun. This gun also demonstrates how rf focusing by altering the gun geometry may be a substitute for traditional emittance compensation using solenoids. Overall, this project represents a significant milestone in the development of sources capable of producing substantial fluxes of narrow-band X-rays with a high brilliance.

ACKNOWLEDGMENTS

Travel to IPAC'17 supported by the Division of Physics of the United States National Science Foundation (Accelerator Science Program) and the Division of Beam Physics of the American Physical Society. This paper is authored by Jefferson Science Associates, LLC under U.S. Department of Energy (DOE) Contract No. DE-AC05-06OR23177. Additional support was provided by DOE Office of Nuclear Physics Award No. DE-SC004094 and Basic Energy Sciences Award No. JLAB-BES11-01. K.D. and J.R.D. were supported at ODU by DO Contract No. DE-SC00004094. This research used resources of the National Energy Research Scientific Center, which is supported by the Office of Science of the U.S. DOE under Contract No. DE-AC02-05CH11231.

REFERENCES

- [1] G. A. Krafft and G. Priebe, Rev. Accel. Sci. Technol. **3**, 147 (2010).
- [2] M. Jacquet, Nucl. Instrum. Methods Phys. Res., Sect. B **331**, 1 (2014).
- [3] G. A. Krafft, E. Johnson, K. Deitrick, B. Terzić, R. Kelmar, T. Hodges, W. Melnitchouk, and J. R. Delayen, Phys. Rev. Accel. Beams **19**, 121302 (2016).
- [4] W. S. Graves, W. Brown, F. X. Kaertner, and D. E. Moncton, MIT inverse Compton source concept, Nucl. Instrum. Methods Phys. Res., Sect. A **608**, S103 (2009).
- [5] *Poisson superfish*, http://laacg1.lanl.gov/laacg/services/download_sf.shtml.
- [6] *Computer simulation technology website*, <http://www.cst.com>.
- [7] J. Qiang, *IMPACT-T User Document Beta Version 1.7*, http://amac.lbl.gov/~jqiang/IMPACT-T/documents/ImpactTv1_7.pdf.
- [8] M. Borland, elegant: A Flexible SDDS-Compliant Code for Accelerator Simulation, Advanced Photon Source LS-287, September 2000.

- [9] A. Michalke, Ph.D. thesis, Bergische Universität Gesamthochschule Wuppertal (1993).
- [10] A. Arnold and J. Teichert, Phys. Rev. ST Accel. Beams **14**, 024801 (2011).
- [11] K. Deitrick, Ph.D. thesis, Old Dominion University, 2017.
- [12] C. S. Hopper, Ph.D. thesis, Old Dominion University, 2015.
- [13] C. S. Hopper and J. R. Delayen, Phys. Rev. ST Accel. Beams **16**, 102001 (2013).
- [14] M. Bech, O. Bunk, C. David, R. Ruth, J. Rifkin, R. Loewen, R. Feidenhans'l, and F. Pfeiffer, J. Synchrotron Rad. **16**, 43 (2009).
- [15] *Lyncean Technologies, Inc. - Synchrotron light and the Lyncean Compact Light Source* <http://www.lynceantech.com/technology.html>
- [16] P. Yu and W. Huang, Nucl. Instrum. Methods Phys. Res., Sect. A **592**, 1 (2008).
- [17] E. G. Bessonov, M. V. Gorbunkov, P. V. Kostyukov, Yu. Ya. Maslova, V. G. Tunkin, A. A. Postnov, A. A. Mikhailichenko, V. I. Shvedunov, B. S. Ishkhanov, and A. V. Vinogradov, J. Instrum. **4** P07017 (2009).
- [18] A. Variola (ThomX Collaboration), in *Proceedings of the 2nd International Particle Accelerator Conference, San Sebastián, Spain* (IPAC'11/EPSC-AG, 2011), p. 1903.
- [19] J. Urakawa, Nucl. Instrum. Methods Phys. Res., Sect. A **637**, S47 (2011).
- [20] R. Hajima, N. Kikuzawa, N. Nishimori, T. Hayakawa, T. Shizuma, K. Kawase, M. Kando, E. Minehara, H. Toyokawa, and H. Ohgaki, Nucl. Instrum. Methods Phys. Res., Sect. A **608**, S57 (2009).
- [21] E. Bulyak *et al.*, Nucl. Instrum. Methods Phys. Res., Sect. A **487**, 241 (2002).
- [22] W. S. Graves *et al.*, Phys. Rev. ST Accel. Beams **17**, 120707 (2014).
- [23] *Beamlines Directory — Advanced Photon Source*, <http://www.aps.anl.gov/Beamlines/Directory/>
- [24] S. Benson *et al.*, Nucl. Instrum. Methods Phys. Res., Sect. A **637**, 1 (2011).